Lifetime studies of self-activated photoluminescence in heavily silicon-doped GaAs

T. Sauncy, C. P. Palsule,* M. Holtz, and S. Gangopadhyay
Department of Physics, Texas Tech University, Lubbock, Texas 79409

S. Massie
Quantum Epitaxial Design, 119 Technology, Bethlehem, Pennsylvania 18015
(Received 22 June 1995; revised manuscript received 18 September 1995)

We report results of a detailed temperature dependence study of photoluminescence lifetime and continuous emission properties in silicon-doped GaAs. The primary focus is on a defect-related emission at 1.269 eV ($T=20$ K). GaAs crystals were grown using molecular-beam epitaxy with most of the experiments conducted on a sample having a carrier concentration of 4.9×10^{18} cm^{-3}. The intensity is seen to decrease above 100 K, with no corresponding decrease in the measured lifetime of 9.63 ± 0.25 ns. The intensity decrease implies an activation energy of 19 ± 2 meV, which is approximately one order of magnitude smaller than what was previously obtained for similar defects in Czochralski-grown GaAs with other dopants. We interpret our results in terms of a configuration coordinate model and obtain a more complete picture of the energy-level structure. The experiments indicate that the upper level in the recombination process is about 20 meV below the conduction-band continuum, with the lower state approximately 300 meV above the valence band. Our results are consistent with the identification of the corresponding defect complex microstructure as being a silicon-at-gallium substitution, weakly interacting with a gallium vacancy second-nearest neighbor, known as the Si-*Y* defect complex.

I. INTRODUCTION

Defects and defect complexes, which occur in heavily doped GaAs (and other semiconductors), have been given much long-term attention, due to their technological relevance and the scientific questions they raise. High dopant concentrations ($>10^{18}$ cm^{-3}) produce defects and defect complexes in sufficient quantity to be significant and to be observed. Most research has focused on isolated point defects and on nearest-neighbor point-defect pairs. Much less has been done on defect complexes involving second-nearest-neighbor point-defect pairs. Recently, two specific defect complexes have been discussed, which appear in moderately to heavily silicon-doped GaAs.[1] These complexes have been put forth as being partially responsible for the reduction of free-carrier concentrations when doping levels exceed $\approx10^{19}$ cm^{-3}.[2]

The first complex currently receiving discussion is denoted Si-*X*, which is believed to involve a silicon-at-arsenic substitution (Si_{As}) and a gallium vacancy (V_{Ga}), possibly stabilized by an arsenic antisite (As_{Ga}).[1] The second defect complex involves a silicon substituting for a gallium (Si_{Ga}) and a gallium vacancy second-nearest neighbor. This is known as the Si-*Y* defect.[3] Recent contributions have been made using infrared absorption (local-mode) spectroscopy to deduce local structure.[1] Photoluminescence (PL) emission studies are also important for examining the influence of defects on optical properties, and how they effect states involved in transport. PL studies can also be used to deduce aspects of the microstructure based on their energy levels, as we do here.

The Si-*Y* defect appears to describe a class of complexes, which all exhibit similar physical properties.[4,5] Specifically, a deep level is common, which gives rise to a PL band near 1.2 eV. This emission is observed in GaAs doped with germanium, tellurium, and tin, as well as silicon.[1] The identification of the defect-related, sub-band-gap PL emission near 1.2 eV as stemming from a vacancy related complex, specifically Si_{Ga}-V_{Ga} in Si-doped GaAs, was first made by Williams.[4]

Recent hydrostatic pressure investigations on heavily silicon-doped GaAs, focused on the 1.2 eV emission band.[6] The pressure measurements showed that the radiative recombination process involves an electronic transition from near the conduction band to the defect level in the gap. Those results are consistent with the Si-*Y* identification, as the source of this band. The purpose of the current work is to further examine and understand the fundamental nature of the near conduction band to defect-level recombination process. To accomplish this, we studied the temperature dependences of the PL intensity in conjunction with recombination lifetime temperature dependence. Our main goal in this paper is to provide more information on the microscopic properties of the defect complex responsible for the emission, and to test for consistency with previous identifications. By correlating the temperature dependence of lifetime and intensity measurements, our results provide a more detailed profile of the energy-level structure and configuration-coordinate diagram, and argue for a self-activated luminescence process.

II. EXPERIMENTAL DETAILS

The samples studied were grown by molecular-beam epitaxy (MBE). Heavily Si-doped GaAs layers were grown (with varying silicon dopant concentrations) on undoped GaAs buffer layers with a substrate temperature of 580 °C. There was no post growth anneal. The substrate was pure liquid encapsulated Czochralski GaAs. The thickness of the doped region varied from sample to sample, ranging from

approximately 2000–6500 Å. Varying the silicon concentrations resulted in free-carrier concentrations ranging from 3.9×10^{17} to 8.6×10^{18} cm^{-3}. The latter were determined by Hall measurements and confirmed with Raman measurements of phonon-plasmon energies.[7] We report here our results from the 4.9×10^{18} cm^{-3} sample only. This sample was singled out because both the band-gap and the defect-related emissions were readily observable.

For all PL measurements, the sample was placed in a closed cycle He refrigerator, with a temperature range of 15 K to room temperature. No attempt was made to shield the sample from outside light during the cooling process, and experiments began from the lowest temperature, while under laser excitation. All continuous-wave (cw) photoluminescence data were recorded using HeNe laser excitation with photon energy 1.96 eV (632.8 nm) and output power of 4 mW. Spectra were dispersed by a 1/4-m double monochromator. An infrared sensitive $In_xGa_{1-x}As$ photomultiplier tube was used for detection of the signal. All spectra were corrected for the wavelength-dependent system response. Time-resolved (TR) spectra were excited using a N_2-pumped dye laser at 2.03 eV (610 nm). Pulse duration was 500 ps, with an average power of 100–150 μJ per pulse at a rate of 10 Hz. A 640 nm cutoff filter was used to eliminate scattered excitation light. The output from the detector was directed to a wave form digitizer and signal averaging was employed (fast analog technique). We used the same spectrometer and detector for both the continuous and time-resolved measurements. Our typical spectroscopic bandpass was 7 meV in the range of the defect emission.

III. RESULTS

A. Temperature dependence of the continuous photoluminescence intensity

We show in Fig. 1 cw spectra taken with the sample at three representative temperatures. In the 20-K spectrum in Fig. 1, three distinct features are seen, denoted A,B, and C for convenience. As shown, all three bands are observable up to 250 K, with B appearing as a weak shoulder. The focus of our current work is band A at 1.269 eV ($T=20$ K). We will first discuss the origins of bands B and C. Band B (1.480 eV at 20 K), appearing only as a shoulder on band C, may be due to band-gap recombination from the GaAs buffer/substrate layer and is not discussed further in this paper. Band C is the band-gap related emission from the doped GaAs. The position and linewidth of this band depend strongly on carrier concentration, due to the Burstein-Moss shift.[8] Our measurements of these bands are consistent with similar MBE-grown GaAs studies.[9]

For examining the temperature dependence of band C in the 4.9×10^{18} cm^{-3} doped sample, no formal peak fitting or line shape analyses were carried out. This band-gap related luminescence has received much attention in the literature, both in theory and in experiment (for example, see Ref. 10) Since this band is not the primary focus of this work, the peak energy position was estimated, and simple analysis is reported as an overall measure of consistency. Bands B and C, as shown in Fig. 1, downshift in energy with increasing temperature, as expected from the shifting of the band gap in pure GaAs.[11] The estimated peak shifts for band C are

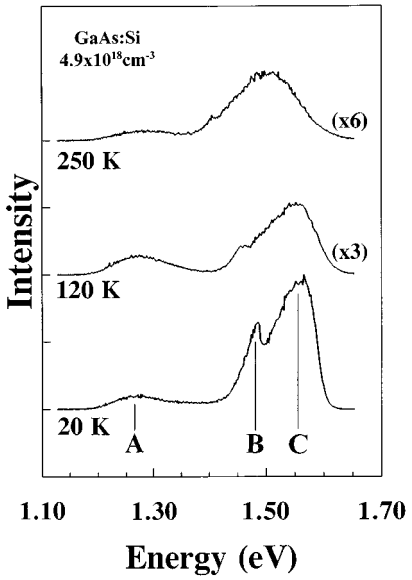

FIG. 1. Three spectra of silicon-doped GaAs, at three representative temperatures, showing the main features discussed in this paper. Peak A is the defect related emission, while B and C stem from band-gap emission of the substrate/cap layer and doped region, respectively.

graphed versus temperature in Fig. 2 (lower). The temperature dependence for this emission energy is fitted well by a quadratic function:

$$E_C=E_0+\alpha T^2, \tag{1}$$

with $E_0=1.550\pm0.001$ eV and $\alpha=-(8.91\pm0.20)\times10^{-7}$ eV/K. This gives, at 300 K,

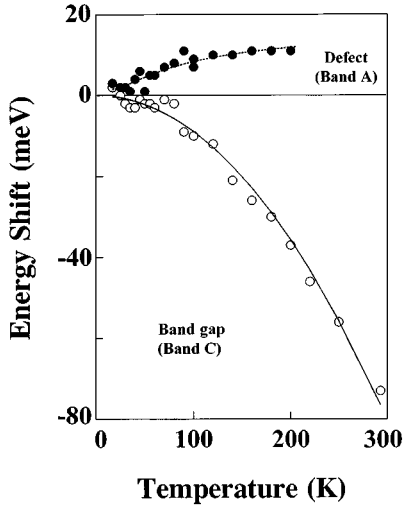

FIG. 2. Temperature induced shift of the estimated peak C maximum for the band-gap related emission (lower), from the extrapolated zero-temperature value of 1.550 eV. The curve is a quadratic fit to the data, Eq. (1) in the text. The upper portion of the graph shows the temperature shift of the defect emission (band A) from the $T=20$ K value of 1.269 eV. Values are taken from Gaussian fits to the data with an error better than ±5 meV.

$$\left[\frac{\partial E_C}{\partial T}\right]_{T=300\ \mathrm{K}} = -0.534 \pm = 0.012\ \ \mathrm{meV/K}, \qquad (2)$$

which compares well with -0.50 meV/K, reported for pure GaAs.[12] Differences arise because of the altered band structure, due to the doping in the GaAs:Si layer and because the position of the Fermi level is temperature dependent.

Band A, the subject of this work, has been identified as near conduction band to defect level recombination.[6] We find that band A exhibits a Gaussian line shape, in agreement with previous studies.[13,14] Fit related errors are approximately ± 1 meV, which is quite likely smaller than the actual precision of our results, but provides some confidence in the overall trends we report. It should be noted here that our measurements of the peak energies differ slightly from those reported elsewhere. Spectra have been corrected for experimentally obtained instrument response. While this has little effect in the energy range of the near-band-gap emission, we found that it is critical when precisely positioning the defect emission, due to the changing response of our system in this energy range. Although a part of this may be due to the quality of the MBE-grown material, the correction of the instrument response also contributes to the difference in emission energy. Our low-temperature linewidths are comparable to those reported by Nguyen *et al.*[14]

Examining the linewidth of the defect emission band, we observe a very weak increase with temperature. Previous analyses of emissions from closely related defects[13] show that this can be described by a configuration coordinate model.[15] According to this model, the linewidth varies as

$$\mathrm{FWHM} = A[\coth(\hbar\omega/2kT)]^{1/2}, \qquad (3)$$

where $\hbar\omega$ represents vibrational energies of the excited state in the emission process. Our results are consistent with this analysis, with $A = 0.103 \pm 0.001$ eV and $\hbar\omega = 44 \pm 5$ meV $= 350 \pm 40$ cm^{-1} from a fit of Eq. (3) to our data. This vibrational energy is higher than what was observed in Te- and Sn-doped GaAs by a factor of ≈ 2.[4] Since silicon local vibrational modes are known to be in this range,[3,16,17] a vibrational energy near 350 cm^{-1}, as implied by our results, is quite reasonable. We will return to this point later.

The peak energy position of band A blueshifts weakly over the temperature range studied, as shown in Fig. 2 (upper). Most of the shifting occurs below 100 K, above which the peak position seems fixed. This behavior has been observed for the related defect emission in both heavily Sn- and Te-doped GaAs.[4] The primary point is that this emission upshifts with temperature, while the band gap is downshifting. This indicates a difference in the effect of temperature on the energy levels responsible for the two emission processes. From our measurements, we estimate the position of the defect ground state level above the valence band shifts from ≈ 280 meV at 20 K to ≈ 204 meV at 250 K.

From analysis of the integrated intensity of band A (from Gaussian fits), we see that the defect-related emission intensity is approximately constant below 100 K, after which it gradually diminishes by a factor of ≈ 8 by 250 K. The trend is analyzed by plotting $\ln(I)$ vs $1/T$, as suggested in the literature.[4,18] In Fig. 3, we can see the intensity behavior described above for the defect. Above ≈ 100 K, the intensity follows an exponential decrease:

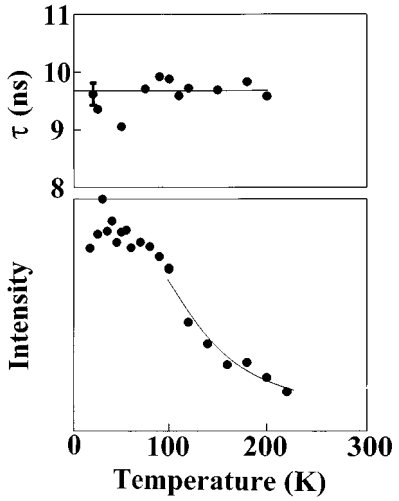

FIG. 3. Temperature dependences of the defect-emission integrated intensity (from Gaussian fits) and total lifetime. The curve in the I vs T portion of the graph shows the exponential decrease above 100 K, as described by Eq. (4) yielding a thermal activation energy of 19 ± 2 meV. Intensity precision is ten percent or better. The upper portion shows that the lifetime is approximately constant over this temperature range with an average value of 9.63 ± 0.25 ns. A typical error bar is shown.

$$I(T) = I_0\ \exp(\Delta E/kT), \qquad (4)$$

where ΔE represents an activation energy for thermal quenching processes. From a least squares fit of the data using Eq. (4), we find $\Delta E = 19 \pm 2$ meV. This activation energy is an order of magnitude smaller than the analogous energy reported for this type of emission in GaAs with Sn and Te dopants.[4] However, our value agrees well with the activation energy found in temperature dependent PL studies involving neutron-transmutation-doped GaAs.[19]

B. Temperature dependence of the defect-emission lifetime

Analysis of the pulsed photoluminescence data was performed by using an iterative reconvolution method, which is described in detail elsewhere.[20] Decay curves were best fitted with the sum of two exponential decays. No improvement was seen by choosing a three life-time fit. The two lifetimes for the measured decay were $\simeq 0.5$ ns and $\simeq 9.6$ ns (20 K). The short lifetime component stems from the tail of band C. Because we measured the defect lifetime at 1.3 eV (due to detector response considerations), band C still has sufficient intensity to contribute to the total signal measured. Time-resolved measurements at the peak of the band-gap related emission confirmed this analysis.

The longer lifetime component is ascribed to the defect-related emission. We, therefore, focus our attention on this lifetime. Data obtained over the 20 to 200 K temperature range are shown in Fig. 3 (upper). Beyond 200 K, extremely weak intensities prevented accurate deconvolution of the decay curves. We see that the lifetime of the defect-related emission is constant, with an average value of 9.63 ± 0.25 ns over this entire temperature range. This is surprising, since the defect-emission intensity is observed to *decrease* above 100 K.

IV. DISCUSSION OF THE RESULTS

The main question to address at this point is the apparent inconsistency between the temperature dependences of the defect-emission intensity and lifetime. The cw integrated intensity of the defect-related emission decreases over the explored temperature range by a factor of ≈ 8, with most of the decrease taking place above 100 K. The lifetime remains constant over the same range. In a two-level system, the total (i.e., measured) lifetime is given by

$$\frac{1}{\tau_{\text{tot}}} = \frac{1}{\tau_{\text{rad}}} + \frac{1}{\tau_{\text{nonrad}}}, \tag{5}$$

where τ_{rad} and τ_{nonrad} are lifetimes for radiative and nonradiative processes, respectively, corresponding to competing recombination avenues, *within* the described system. From Fig. 3, we see that the measured lifetime does not change with temperature.

Continuous-wave intensities are proportional to the number of electron-hole pairs available to participate in the recombination, times the ratio of the total lifetime to the radiative lifetime. Therefore, along with the decrease in cw intensity, one would expect a corresponding decrease in the observed lifetime. Decreases in the observed lifetime with temperature are generally attributed to increasing competition from nonradiative transitions between the initial and final levels. This observation, in light of Eq. (5), suggests that the temperature-dependent nonradiative processes [represented by τ_{nonrad} in Eq. (5)] are not competing on the same time scale with the radiative process responsible for the defect emission. Considering more complicated processes (e.g., a three-level system) does not clarify the analysis.

Evidently, the observed decrease in the cw intensity of the defect emission over this temperature range stems from a decrease in the number of available electron-hole pairs. This decrease in the number of available carriers may be due to thermal activation of electrons from the upper level (into the conduction-band states) or holes out of the defect-level ground state (into the valence-band state), or a combination of both, competing with the thermalization of carriers. The activation energy, $\Delta E = 19 \pm 2$ meV, associated with the thermal quenching of the cw intensity is more than one order of magnitude smaller than the energy spacing between the ground state of the defect complex and the valence-band maximum (over the entire temperature range studied). This suggests that depletion of holes from the defect level to the valence band is not the primary cause of the decrease in the available electron-hole pair population. Rather, the decrease is a result of the thermal activation of electrons from a level that is discrete and lies $\sim \Delta E$ below the conduction-band states. These two processes, i.e., thermalization and reactivation of electrons, are very fast processes taking place on the same time scale ($\sim$ps), so they compete with each other, effectively reducing the number of electrons trapped in the upper level of the defect complex. The defect recombination, which is much slower than these two processes, still takes place in the same manner as at lower temperatures without any competing processes on its time scale. The excess holes trapped on the vacancies may recombine with excess conduction band electrons subsequently via nonradiative transitions, which are slower than the defect recombination. Since these transitions are slower, they do not affect the lifetime of the defect recombination process according to Eq. (5).

The close proximity of the upper defect level to the conduction continuum is in agreement with what was observed under pressure: the direct to indirect crossover occurs at 4 GPa.[6] This is the pressure at which the conduction-band minima cross (direct to indirect), making transitions from the X point energetically favorable for radiative recombination. Even though it is still present for pressures higher than 4 GPa, the defect excited state has shifted above the X minimum. Electrons will favor thermalizing into the X well minimum before radiatively decaying into the lower defect level. A crossover pressure appreciably higher (lower) than 4 GPa would signal an upper state well below (above) the lowest conduction-band states, but that is not the case here.

At this point,we need to put our results into context with the prevailing defect microstructure associated with this subband-gap emission, and test for consistency. This defect complex is believed to consist of a gallium vacancy (acceptorlike) interacting with a substitutional silicon at gallium (donorlike). In GaAs, the isolated silicon donor level is located 5.8 meV below the conduction band.[21] From the thermal quenching of the photoluminescence intensity data, we propose that the upper (photoexcited) state of the defect complex appears to lie $\simeq 20$ meV below the conduction-band continuum. This 20 meV value does not take into account any offset, due to zero-point vibrational motion. The ground state of the defect would, therefore, consist of an electron wave function, which is spatially shifted toward the gallium vacancy, since it is slightly positive. This is approximately 1.2 to 1.3 eV below the conduction band or 0.2 to 0.3 eV above the valence band. This is close to the deep level associated with an isolated V_{Ga}^{-} in GaAs.[22]

In our case, several factors alter the energy levels associated with the isolated point defects. The primary factor is the Coulomb interaction between the vacancy and the silicon atom, and the resultant distortion surrounding the complex. The excited state then corresponds to the first excited state of the defect complex for which the single-electron wave function is spatially biased toward the Si_{Ga} atom. This corresponds loosely to the isolated silicon donor level. This is also consistent with the pressure studies, since shallow donors (acceptors) are known to shift rigidly with the conduction (valence) band.[23,24] Both the V_{Ga} and Si_{Ga} will be approximately neutral in the excited state of the complex. In the ground state of our emission process, the *net* complex is charge neutral and is best approximated by V_{Ga}^{-} and Si_{Ga}^{+} for representing the charge distribution. This picture implies consistency between our results and the Si_{Ga}-V_{Ga} defect.

The entire photoluminescence picture proposed here is as follows. Holes are first produced in the defect complex by one of two processes. Incident photons are absorbed by promoting electrons out of the defect complex ground state [process A in Fig. 4(a)] or out of the valence band (not shown). In the latter, holes can thermalize into the defect level. In either case, the defect complex becomes positively charged. Second, process B in Fig. 4(a) shows the defect complex capturing an electron, most likely from the ample number of electrons present in the conduction band due to doping. This leaves the defect neutral, but in its first excited state, which is a silicon donorlike level. The step observed is the radiative

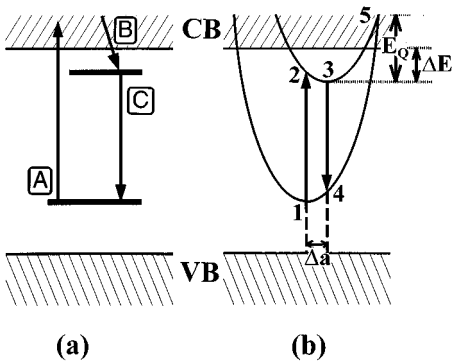

FIG. 4. Energy band schematics (not to scale) deduced from our results. Part (a) shows the simplest photoluminescence process responsible for the observed band A (transition C). In (b), we show the configuration coordiate diagram, which describes our results for the self-activated photoluminescence of the defect complex. The intensity reduction seen in Fig. 3 stems from thermal activation of electrons out of the defect upper energy level into the conduction continuum states.

transition of the excited electron back into the ground state, represented by step C in Fig. 4(a). Finally, the defect complex relaxes causing a volume deformation. This type of ''self-activated'' luminescence has been reviewed by Shionoya for defects in ZnS (Ref. 25) and later extended to defects in III-V compounds. (For example, see Ref. 4.)

We believe this recombination process to be essentially ''molecular,'' which can now explain the temperature dependences of the lifetime and cw intensity. The lifetime is constant, because it corresponds to an intradefect electron recombination [step C in Fig. 4(a)]. This suggests that the defect only interacts weakly with the surrounding lattice. The weak temperature dependence of the cw emission linewidth, which implied a vibrational interaction energy of 44 ± 5 meV $=350\pm40$ cm^{-1} supports this point. This value is in approximate agreement with a previous report.[19] Although the value obtained from our analysis should not be overinterpreted, it does make sense, as it spans a range corresponding to silicon local-mode vibrational energies. These vibrational modes can serve to promote electrons from the weakly localized upper level of the defect complex into the conduction-electron continuum, which appears to be 20 meV away. The cw intensity of the defect emission decreases above 100 K, due to the close proximity of the first (neutral) excited state with the conduction states. As temperature increases, local-mode vibrations become more plentiful and eventually serve to promote electrons upward making them unavailable for the *intradefect PL* process. The nonradiative thermalization and reactivation processes are extremely fast, corresponding to phonon lifetimes ($\approx$ps). Once liberated into the conduction band, the electron can then lose its excess energy. This can happen by band-gap recombination or nonradiative processes. Nonradiative transitions are enhanced by the existence of a nonzero density of states throughout the gap, a result of the presence of defects. The electron then no longer plays a role in the defect emission process. This accounts for the decreasing intensity that we observe for the defect luminescence above 100 K without a decrease in total lifetime.

Previous analysis of the defect-emission process relied on configuration coordinate (CC) diagrams (see Ref. 15). In Fig. 4(b), we show a schematic of the CC model as applied to our interpretation of the current results. We observe emission, due to the transition of an electron from point 3–4 in the figure. It has been proposed that the activation energy inferred from the intensity measurements was representative of the energy of the avoided crossover point of the upper (excited) and lower (ground) CC curves, relative to the minimum of the upper curve [shown as E_Q in Fig. 4(b)]. In this interpretation, given an amount E_Q of thermal energy, an electron will transfer from the ''upper'' CC to the ''lower'' CC at point 5 in Fig. 4(b). These electrons will then nonradiatively work their way to point 1 of the diagram. The result is thermal quenching of the intensity with an activation energy of E_Q. This previous interpretation also implies a temperature dependence of the lifetime, since this nonradiative process would be on a similar time scale, and involve the same intradefect initial state, as the radiative process. The measured lifetime would depend on temperature according to[15]

$$\frac{1}{\tau(T)}-\frac{1}{\tau_L}=Se^{-E_Q/kT}, \tag{6}$$

where τ_L is the *measured* lifetime at a temperature below which thermal quenching is negligible (here $\geqslant$100 K) and S is a temperature-independent prefactor, which is typically determined by fitting Eq. (6) to the data. The lifetime that we measured for the defect-related emission does not exhibit this temperature dependence.

As mentioned, previous estimates of E_Q were approximately one order of magnitude larger than our $\Delta E\simeq20$ meV. The much larger values were obtained for GaAs, with dopants other than Si, such as Sn and Te,[4] the chemical tendencies of which differ from those of Si. The positions of the energy levels, which form in the gap due to a defect complex, may shift for different dopants, while still producing the observed luminescence band at $\approx$1.26 eV. Crystal quality of the samples used in the previous studies could be critical, along with the fact that other species imply a variety of local environments. All of these factors may contribute to differences in the temperature dependence of the emission. This difference needs to be examined further, and motivates experiments on MBE grown GaAs with high concentrations of these dopants. Our results do not invalidate the CC model as applied to defect complexes, especially when applied to defects for which both ground and excited states are deep within the energy gap. However, the lifetime model [Eq. (6)] developed based on the previous determination of E_Q, when applied here, results in a temperature dependence we do not observe. We believe, as discussed, that the 20 meV value corresponds to the depth of the first excited state from the conduction continuum states. We point out that the temperature-dependent lifetime studies, which provide a different approach to the analysis of these processes, have proven to be instrumental in developing a more complete picture.

We address now the possibility that the defect emission that we study is related to other defects, which may be present in doped GaAs. Especially tempting is any possible link with the DX center. This link is suggested by the fact

that sub-band-gap emission, near 1.26 eV, has been observed in n-type GaAs when doped with Si, Sn, Te, S, and Se,[4] each of which has exhibited DX behavior (under the correct conditions).[26] Since the material that we investigate allows for a variety of defect structures, including DX, we must recognize that other defects may play a secondary role in the intensity decrease we observe above ≈100 K. However, the circumstances in which we place our samples for the current studies are not favorable for forming DX centers, so that we do not expect it to play a role. Further experiments, possibly in $Al_xGa_{1-x}As$, aimed at linking the 1.25 eV band and the existence of DX behavior, would be necessary to establish any such connection.

Finally, some mention of the charge capture volume deformation is in order. The (absolute) pressure coefficient of the defect level has been shown to be useful for estimating the net volume deformation of point defects upon charge capture (V_c) or emission.[27] For this defect complex, similar analysis yielded $V_c = +2.7 \pm 0.63$ Å^3.[6] This value for volume deformation is comparable to that for the $EL2$ defect (upon charge capture) in GaAs, reported by Samara *et al.*,[27] and for DX center (upon emptying) in Sn- and Si-doped GaAs, reported by Cargill *et al.*[28] However, the meaning of charge capture is somewhat obscured, because we now view the emission process as involving the intradefect transfer of an electron abbreviated by $(Si_{Ga}{}^0 - V_{Ga}{}^0) \rightarrow (Si_{Ga}{}^+ - V_{Ga}{}^-)$. The complex as a whole remains charge neutral. Charge capture in this case is the removal of an electron from the neutral Si_{Ga} to the vacancy. The above volume deformation corresponds to the expansion of the entire defect complex volume, due to the emission process [point 4–1 in Fig. 4(b)]. If we consider the defect volume to be ≈1/4 the unit cell volume, this implies a linear deformation of approximately $\Delta a \simeq 0.1$ Å. The value of Δa should be on the order of the displacement reflected in the CC diagram in Fig. 4(b). A similar value is obtained using the analysis laid out in Ref. 29, by using parameters obtained in fitting the temperature dependence of defect-emission linewidth.[30] Our value for Δa is appropriate for weak defect-lattice interaction. Theoretical studies of second-nearest-neighbor defect complexes involving Si_{Ga} are consistent with our conclusion of a weakly interacting point defect-host system.[31] Further exploration of this type of analysis is needed to develop its power for determining characteristics of defect microstructures.

V. SUMMARY

By correlating the measured temperature dependences of the cw intensity and lifetime of the vacancy related emission near 1.269 eV, we construct a more complete picture of the energy-level structure of the process. Results are summarized in Fig. 3 and the energy-level and CC diagrams are depicted in Fig. 4. The integrated intensity is seen to diminish by a factor of ≈8 in the 20 to 250 K range, with nearly constant intensity to 100 K. However, the lifetime remains constant at an average value of 9.63 ± 0.25 ns to 200 K. This tells us that there are no intradefect nonradiative processes competing on the same time scale with the observed emission. This implies that the intensity decrease must be due to thermal depletion of electrons or holes from the levels that participate in the observed radiative recombination.

The temperature dependence of the cw emission integrated intensity implies a thermal activation of 19 ± 2 meV. This is consistent with previous hydrostatic pressure experiments on the same samples.[6] Our activation energy is approximately one order of magnitude smaller than those obtained in earlier studies on Czochralski grown GaAs with other dopants.[4] We believe this to be attributable, in part, to the crystal quality obtainable using MBE growth. We interpret our activation energy as a signature of the depth of the upper defect level from the conduction levels, rather than of a crossover to the lower curve of the CC model [Fig. 4(b)]. Evidently, depletion (reduced cw intensity) is a consequence of a competition between thermalization and reactivation of electrons out of the upper defect level, which is located ≈20 meV below the conduction continuum states. The excess holes subsequently recombine with the excess conduction-band electrons nonradiatively.

We analyze our results in the context of the Si-Y defect, plausibly identified as a Si_{Ga}-V_{Ga} second-nearest-neighbor complex. The defect appears to interact only weakly with the lattice, as evidenced by the very small temperature dependence of the linewidth. Furthermore, the silicon and vacancy comprising the complex only weakly influence each other: the lower state closely resembles the isolated gallium vacancy and the upper state is close to an isolated silicon donor level. Recombination is intradefect or self-activated and is consistent with the measured constant lifetime.

It would be important at this stage to conduct the complementary excitation spectroscopy measurements to attempt to precisely determine those optical excitations, which are responsible for this emission [1–2 in Fig. 4(b)]. This would permit a better construction of the CC diagram through determination of the Franck-Condon shift. These measurements are currently in preparation.

ACKNOWLEDGMENTS

The authors wish to thank R. C. Newman for helpful discussions and critical reading of this manuscript. T.S. gratefully acknowledges that this material was supported by the National Science Foundation. C.P.P. was supported (in part) by Texas Tech Center for Energy Research.

*Present address: University of Oregon, Eugene, OR 97403.

[1] R. C. Newman, Semicond. Sci. Technol. **9**, 1749 (1994).
[2] J. Maguire, R. Murray, and R. C. Newman, Appl. Phys. Lett. **50**, 516 (1987).
[3] S. A. McQuaid, R. C. Newman, M. Missous, and S. O'Hagan, Appl. Phys. Lett. **61**, 3008 (1992).
[4] E. W. Williams, Phys. Rev. **168**, 922 (1968).
[5] H. Shen, G. Yang, Z. Zhour, W. Huang, and S. Zou, J. Appl. Phys. **68**, 4894 (1990).
[6] M. Holtz, T. Sauncy, T. Dallas, and S. Massie, Phys. Rev. B **50**, 14 706 (1994).
[7] A. Mooradian and G. Wright, Phys. Rev. Lett. **16**, 999 (1966).
[8] E. Burstein, Phys. Rev. **93**, 632 (1954); T. S. Moss, Proc. Phys. Soc. London Sect. B **76**, 775 (1954).

[9] Jiang De-Sheng, Y. Makita, K. Ploog, and H. J. Queisser, J. Appl. Phys. **53**, 999 (1982).
[10] A. Haufe, R. Schwabe, H. Fieseler, and M. Ilegems, J. Phys. C. **21**, 2951 (1988).
[11] M. D. Sturge, Phys. Rev. **127**, 768 (1962).
[12] J. I. Pankove, *Optical Processes in Semiconductors* (Dover, New York, 1971).
[13] H. Barry Bebb and E. W. Williams, in *Transport and Optical Phenomena*, edited by R. K. Willardson and A. C. Beer, Semiconductors and Semimetals Vol. 8 (Academic, New York, 1972), Chaps. 4 and 5.
[14] Nguyen Hong Ky, L. Pavesi, D. Arajo, J. D. Ganiére, and F. K. Reinhart, J. Appl. Phys. **69**, 7585 (1991).
[15] C. C. Klick and J. H. Schulman, in *Solid State Physics: Advances in Research and Applications*, edited by F. Seitz and D. Turnbull (Academic, New York, 1957), Vol. 5, p. 97.
[16] W. M. Theis and W. G. Spitzer, J. Appl. Phys. **56**, 890 (1984).
[17] M. Holtz, R. Zallen, A. E. Geissberger, and R. A. Sadler, J. Appl. Phys. **59**, 1946 (1986).
[18] T. Koda and S. Shionoya, Phys. Rev. **136**, A541 (1964).
[19] M. O. Manasreh and S. M. Mudare, Semicond. Sci. Technol. **4**, 435 (1989).
[20] C. P. Palsule, S. Gangopadhyay, A. Kher, and W. Borst, Phys. Rev. B **47**, 9309 (1993).
[21] S. M. Sze, *Physics of Semiconductor Devices* (Wiley, New York, 1981), p. 21.
[22] H. Xu and U. Lindfelt, Phys. Rev. B **41**, 5979 (1990).
[23] D. J. Wolford and J. A. Bradley, Solid State Commun. **53**, 1069 (1985).
[24] A. Zylberstejn, R. H. Wallis, and J. M. Besson, Appl. Phys. Lett. **32**, 764 (1978).
[25] S. Shionoya, in *Luminescence of Inorganic Solids*, edited by P. Goldberg (Academic, New York, 1966), pp. 225–286.
[26] P. M. Mooney, J. Appl. Phys. **67**, R1 (1990).
[27] G. A. Samara, D. Vook, and J. F. Gibbons, Phys. Rev. Lett. **68**, 1582 (1992).
[28] G. S. Cargill, A. Segmüller, T. F. Kuech, and T. N. Theis, Phys. Rev. B **46**, 10 078 (1992).
[29] R. K. Watts, *Point Defects in Crystals* (Wiley, New York, 1981), pp. 86–106.
[30] We use a nominal phonon frequency of 300 cm^{-1} to derive an order of magnitude force constant for this calculation.
[31] R. Jones and S. Öberg, Semicond. Sci. Technol. **9**, 2291 (1994).